DETERMINING THE MECHANISM OF SV40-INDUCED DNA DAMAGE

By

Weston Dulaney

Thesis

Submitted to the Faculty of the

Graduate School of Vanderbilt University

In partial fulfillment of the requirements

for the degree of

MASTER OF SCIENCE

in

Biological Sciences

May, 2011

Nashville, TN

Approved:

Ellen Fanning

Katherine Friedman

TABLE OF CONTENTS

LIST OF FIGURES

CHAPTER I

INTRODUCTION

Simian Virus 40

Capsid structure

Simian virus 40 (SV40) is a small nonenveloped virus of the *Polyomaviridae* family. Three structural proteins compose the SV40 capsid: VP1, VP2, and VP3. The principal protein that forms the capsid is VP1. Cryo-electron microscopy and crystallographic studies have provided a wealth of structural information on the arrangement of VP1 in the SV40 capsid (5, 6, 43, 74; figure 1.1). Seventy two copies of the VP1 pentamer are arranged into an icosahedral capsid. Twelve of the 72 pentamers are coordinated by five other pentamers; each of the other 60 pentamers are coordinated by six pentamers. Adjacent pentamers are held together by intermolecular VP1 disulfide bonds. The viral genome, along with the other two structural proteins, VP2 and VP3, remains encapsidated until the viral uncoating begins.

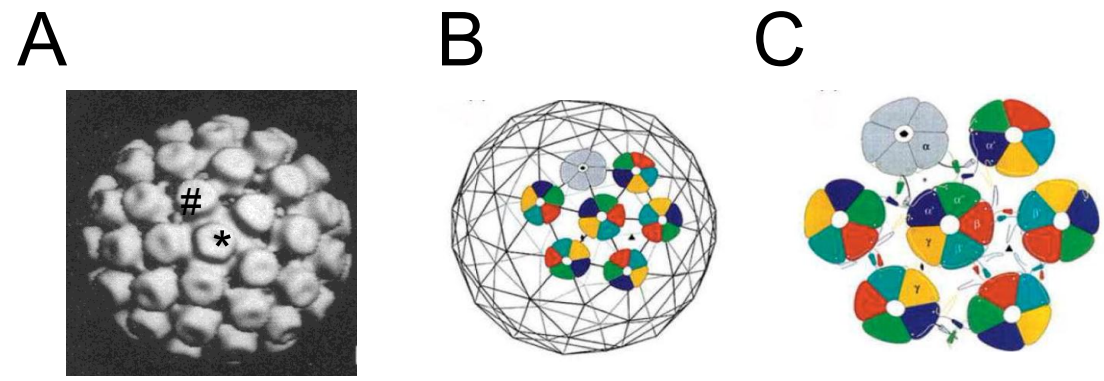

Figure 1.1. Structure of the SV40 capsid. A. Low resolution three-dimensional reconstruction of the SV40 capsid obtained from cryo-electron microscopy. The capsid is projected down the 5-fold icosahedral axis. The corresponding 5-coordinated pentamer is denoted with an asterisk. An example of a 6 coordinated pentamer is denoted with a pound sign (modified from ref 6.) **B.** Arrangement of VP1 pentamers in the SV40 capsid (figure from ref. 74). **C.** The organization of the SV40 intermolecular disulfide bonds at a 6-coordinated pentamer (figure from ref. 74).

Genome organization

The SV40 genome is a 5.2 kb circular double stranded DNA molecule that is packaged with host histones. Sections of the genome are classified according to the time during infection genes are expressed. Expression of the early genes: (large tumor (T) antigen, small t-antigen, and 17k t-antigen) begins 8-10 hours post infection (hpi). A viral microRNA is also part of the early viral transcripts that acts in a negative feedback loop to repress early gene expression (75). Expression of the late genes results in the structural proteins VP1, VP2, and VP3. Agnoprotein is produced from a third late open reading frame and functions in SV40 virion assembly and maturation (36).

T-antigens

Polyomavirus T-antigens are responsible for cellular transformation and genome amplification. Large T-antigen (Tag) transforms host cells by disrupting functions of p53 and pRb, regulators of cell cycle progression. Tag physically interacts with p53, preventing its involvement in activating cell cycle checkpoints (2). Tag also brings together a heat shock chaperone 70 with complex pRB-E2Fcomplexes. Tag stimulates chaperone activity of Hsc70 to disrupt the pRb-E2F complex, thereby stimulating E2F transcription activity (2). Through these mechanisms, Tag disrupts cell cycle control forcing the host cell into an S-phase state (40). The Tag protein is also directly involved in viral genome amplification. Tag binds to the SV40 origin sequences, unwinds DNA, and recruits host DNA replication proteins, including DNA polymerase α-primase (pol-prim), the processive polymerase δ, and the ssDNA binding complex replication protein A (RPA). *In vitro* studies of SV40 replication DNA replication using purified proteins have revealed many insights into eukaryotic DNA replication protein dynamics (20). Small t-antigen also contributes to cellular transformation by inhibiting protein phosphatase 2A, a ubiquitous serine-threonine protein phosphatase (4).

SV40 cell entry

In order to enter its host cell, SV40 binds to GM1 ganglioside receptors and initiates caveolin-mediated endocytosis (60, 78). Caveolin is not an essential part of the endycytosis program, as SV40 can successfully enter cells lacking caveolins (16). The only structural protein required to initiate endocytosis

is VP1, as it directly interacts with the carbohydrate moiety on the GM1 receptor (53, 56). After internalization into caveolae, virions are first trafficked to caveosomes, large pH neutral membranous organelles, between 0-1 hpi. Small caveolin-free vesicles bud from the caveosome and move by microtubule-dependent transport into the smooth endoplasmic reticulum (ER), where virus particles accumulate by 4-6 hpi (34, 60). The order of events in entry that follows is shared by a variety of polyomaviruses (55). SV40 has presumably evolved to target the ER to take advantage of protein disulfide isomerases that initiate viral uncoating. In this process, intermolecular disulfide linkages in the outer capsid protein VP1 are reduced and reoxidzed to intramolecular bonds. This isomerization reaction allows capsid destabilization, as reflected in release of 20% of VP1 pentamers that correspond to those at the twelve five-coordinated vertices of the icosahedron (69).

In order to exit the ER, SV40 and other polyomaviruses utilize the retrotranslocation machinery associated with the ER-associated degradation (ERAD) pathway (79; figure 1.2). When sensors in the ER indicate an excess of improperly folded protein, retrotranslocation channels are used to transport proteins into the cytoplasm for degradation (65). Knockdown of Derlin-1, a component of the retrotranslocon, inhibits SV40 infection (69). Similarly, disrupting retrotranslocon function through expression of a dominant-negative Derlin-1 protein inhibits BKV infection (33). An alternative way in which polyomavirus capsids or genomes may exit the ER is proposed to involve construction of a viroporin containing VP2 and VP3, structural proteins that

emerge after partial uncoating in the ER (17, 62). The most clearly characterized role that VP2 and VP3 play is delivering the SV40 genome to the nucleus. VP3 contains a nuclear localization signal that binds to importins that and is used to move the SV40 minichromosome into the nucleus (52, 54).

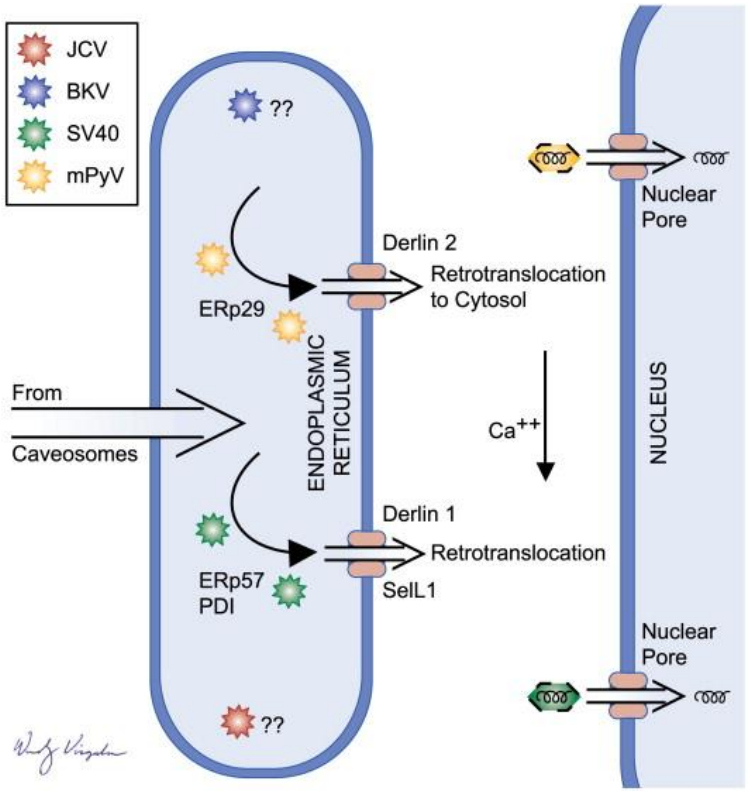

Figure 1.2. Polyomavirus trafficking during cell entry. SV40, JCV, BKV, and mouse polyomavirus (mPyV) enter the endoplasmic reticulum from caveosomes. Different ER proteins are retrotranslocation of each polyomavirus. (Figure from ref. 55)

Polyomaviruses and Human Health

SV40 is a well studied virus that permissively infects monkey kidney cells. The best studied human polyomaviruses are the JC and BK viruses. These viruses were named during their discovery using the initials of the patients from whom the viruses were first isolated (22, 58). Typically replication of these viruses is detectable only during extreme immunosupression, as with administration of steroids to organ transplant patients. When reactivated, BKV can result in severe nephropathy and JCV is associated with progressive multifocal leuokoencephalopathy.

New human polyomaviruses are still being uncovered. Two recently isolated examples of human polyomaviruses are the Washington University virus (WUV; 3) and Karolinska Institutet virus (KIV; 23) which were named for the institutions at which they were isolated. WUV or KIV has not yet been clearly associated with disease states. One of the most interesting new polyomaviruses that is correlates with a disease state is Merkel cell polyomavirus (MCV), which was identified due to its association with a rare skin cancer that affects immunocompromised patients (21). JCV and BKV are genetically more closely related to SV40 than the emerging polyomaviruses (15). A recent estimate of the seroprevalence of polyomaviruses in the United States indicates that 15-82% of healthy persons are seropositive for one of the human polyomaviruses (35). Because a high percentage of the population has been exposed to these poorly classified microbes, some with unknown pathogenicity, research on polyomaviruses still has high significance in human health.

Polyomavirus Interactions with DNA Damage Signaling Pathways

DNA damage reponse

Several complex signaling cascades have evolved in eukaryotes to guard against genome instability (32). The DNA damage response comprises three major pathways regulated by ataxia telangiectasia mutated (ATM) kinase, ATM and Rad3 related (ATR) kinase, and the DNA dependent protein kinase (DNA-PK). When activated by double strand breaks, ATM phosphorylates histone H2AX on Ser139 in humans (γH2AX), which helps to recruit repair proteins to the DNA lesion and activates checkpoint signaling to prevent cell cycle progression (38). ATR primarily responds to DNA lesions associated with stalled replications forks that are recognized by extended exposure of RPA-coated single-stranded DNA (12). DNA-PK has many substrates that overlap with ATM and ATR and has the unique function of initiating the nonhomologous end joining repair mechanism (31).

The host DNA damage response supports polyomavirus infection

Viruses have evolved in some cases to suppress the cellular DNA damage response, whereas others activate and exploit DNA damage signaling to facilitate viral replication (81). Polyomaviruses activate DNA damage signaling and exploit this signaling which plays a key role in their replication. Mouse polyomavirus (MPy) activates the ATM pathway, and the PI3K inhibitor caffeine

reduced viral propagation and viral DNA synthesis (14). Similarly, in SV40-infected CV-1 cells, ATM is robustly activated by 24 hpi and phosphorylates its downstream targets in SV40 infected CV-1 cells. Knockdown of ATM using siRNA lowers viral DNA synthesis in infected cells (72). ATM also phosphorylates SV40 Tag, but the function of the posttranslational modification remains unclear (72). The ATR pathway also participates in the SV40 life cycle by manipulating p53 to maintain an S-phase environment suitable for viral DNA replication and modulating the phosphorylation state of pol-prim (64). It has been suggested that DNA-PK is activated during SV40 infection and is important for modifying p53 (64), but direct evidence for this is lacking.

By studying the subcellular localization of ATM substrates in SV40-infected BSC40 cells, the Fanning lab previously found that large nuclear foci formed 24 hpi in which a number of host DNA replication and repair proteins colocalize with Tag (86). Additionally, a specific small molecule inhibitor of ATM limited viral DNA production in BSC40 cells and disrupted assembly of viral replication centers (86). Taken together, ATM signaling appears to promote organization of subnuclear sites of viral genome duplication, as is the case for herpes simplex virus (44), human papillomavirus (51), minute virus of mice (1), and minute virus of canines (47).

Thesis Organization

This thesis reflects the combined efforts of Dr. Xiaorong Zhao, a former postdoc in the lab, her undergraduate students Becky Lou and Kathryn

McCreless, and myself. Chapter 2 consists of materials and methods used throughout chapters 3 and 4. Chapter 3 consists of preliminary data collected by X. Zhao, B. Lou, and K. McCreless before I began working on this project. Chapter 4 includes data that is the result of my research in the Fanning lab. Chapter 5 is a discussion of the data found in chapters 4 and 5.

CHAPTER II

MATERIALS AND METHODS

Propagation of SV40 and Determination of Titer

Initial stocks of SV40 were obtained from the laboratory of Jim Pipas at the University of Pittsburgh. New stocks of SV40 were prepared by infecting T150 flask with confluent BSC40 cells at an MOI of 0.1. Infection was allowed to proceed for 48 hours, fresh DMEM was added, and infection was allowed to proceed for another 40-48 hours. At this time, flasks were frozen and thawed to room temperature 3 times. The cell pellet was spun down at 1000 rpm for 5 minutes. The supernatant containing SV40 was stored at -80˚C. To determine the titer of the virus, serial 1:10 dilutions were prepared of the virus stock of . Then, 0.5 mL of each dilution was used to infect confluent BSC40 cells in 6 well plates. Cells were fixed at 24 hpi, permeabilized, and immunofluorescently stained for Tag using the protocol found below in the Indirect Immunofluorescence section below. Confocal microscopy was used to determine the highest dilution that still contained infected cells, typically in the range of 1-10 infected cells per slide. To determine titer, this number is multiplied by two to account for the use of 0.5 mL to infect the cells and divded by the dilution. For example, if one infected cell is found on the 10^{-7} infection, the titer is 2×10^{7} pfu/mL.

Cell Culture and Virus

BSC40 cells were maintained in Dulbecco's modified Eagle's medium (DMEM) supplemented with 10% fetal bovine serum (FBS) and 2 mM L-glutamine. SV40 stocks with a titer of 2 x 10^7 pfu/mL were used for infections. Cells were infected by adding SV40 at the indicated multiplicity of infection (MOI) at 0 hpi with DMEM without FBS at a total volume of 500 µL in 35 mm tissue culture dishes. This volume was scaled according to surface area of the dish in the case of using size dishes. Dishes were rocked to redistribute the virus over the cells every 15 minutes for the first 2 hours. At this time, the media containing virus was aspirated and replaced with warm supplemented DMEM. To UV irradiate SV40, a small volume of virus was placed in a sterile tissue culture dish and irradiated in a UV Stratalinker 1800 (Stratagene) for 5 minutes using the time setting.

Drugs

Neocarzinostatin at 0.5 mg/mL in pH 6.0 MES buffer (Sigma) was diluted to 50 ng/mL in DMEM and cells were treated15 min to induce DNA damage. Thapsigargin at 2 mM in DMSO (Fisher ICN15899901) was diluted at 2 µM in DMEM for 12 hr. The following drugs were added to cell culture medium during SV40 infections at 2 hpi to avoid interference with cellular uptake of virus: 10 mM or 40 mM N-acetyl-L-cysteine diluted from 1 M stock in water (63; Sigma), 250 µM or 5 µM Nocodazole diluted from 1 mg/mL stock in DMSO (69; VWR), 5 mM dithiothreitol diluted from 1M stock in water (DTT; 69; RPI), 100 µM 1,2-bis(o-

aminophenoxy)ethane-N,N,N',N'-tetraacetic acid acetoxymethyl ester from 10 mM stock in DMSO (80; BAPTA-AM; Invitrogen), 100 nM Ru-360 from 100 µM stock solution in DMSO (42; Calbiochem).

Indirect Immunofluorescence

At the indicated time points, cells were washed in phosphate buffered saline (PBS), then in cytoskeleton (CSK) buffer containing containing 10 mM PIPES (pH 6.8), 100 mM NaCl, 300 mM sucrose, 1 mM $MgCl_2$, and 1 mM EGTA. Soluble proteins were then pre-extracted for 4 min on ice in CSK buffer containing 0.5% Triton X-100, 0.15 µM aprotinin, 1 mM PMSF, and 1 µM leupeptin and fixed for 10 min in 4% paraformaldehyde in PBS. After fixation, cells were washed three times in PBS, incubated for 20 min with Image-iT (Invitrogen), washed in PBS, and blocked with 10% fetal bovine serum (FBS) in phosphate buffered saline (PBS). Primary antibodies, mouse anti-γH2AX (Upstate 05-636) and rabbit anti-Tag, were applied in 10% FBS in PBS for 45 min at 37º. Dilutions for primary antibodies were 1:1000 mouse anti-γH2AX and 1:2000 for rabbit anti-Tag. Cells were washed three times in PBS with 0.05% Tween-20 (PBST). Secondary antibodies, donkey anti-mouse Alexa 488 and donkey anti-rabbit Alexa 555 (Invitrogen), were added in 10% FBS in PBS for 45 min at 37º. Cells were washed three times in PBST. Nuclear counterstain was performed by incubating cells with 0.33 µM TO-PRO-3 iodide (Invitrogen) in PBS for 20 min at room temperature.

Western Blotting

Cell lysate was prepared by adding 200 µL of lysis buffer (HEPES pH 7.3, 250 mM NaCl, 0.1% NP-40, 10 mM NaF, 0.3 mM Na_3VO_4, 0.15 µM aprotinin, 1 mM PMSF, and 1 µM leupeptin) to a confluent 60 mm dish and removing cells with a cell scraper. Protein concentration of cell lysates was assayed as per manufacturer's protocol using a bicinchoninic acid kit (Pierce) and equal amounts of total protein were loaded into an acrylamide gel and separated using SDS-PAGE. The amount of protein for each experiment loaded in each lane varied between 1-2 µg. Proteins were transferred to nitrocellulose in bicarbonate buffer (18) and blocked in 5% nonfat dry milk in tris buffered saline with Tween-20 (TBST). Primary antibodies, anti-Tag (Pab101) and mouse anti-Tubulin (Santa Cruz SC-5286), and mouse anti-IκB-α (Santa Cruz SC-203) were added in 1% milk in TBST overnight at 4º. Dilutions for primary antibodies were 1:1000 for Pab101, 1:200 for mouse anti-tubulin, and 1:200 for mouse anti- IκB-α. After washing in TBST, HRP-conjugated secondary antibodies were added at 1:5000 dilution in 1% milk in TBST. Membranes were developed using an ECL kit (Pierce) and exposed to film. Bands were quantified using Bio-Rad Quantity One software.

Single Cell Gel Electrophoresis Assay

A Comet assay kit (Trevigen) was used to prepare cells for single cell gel electrophoresis according to manufacturer's instructions. Briefly, cells were harvested by trypsinization, suspended in low melting agarose (Trevigen) and

plated on Comet slides. Slides were treated with alkaline solution (300 mM NaOH, 1 mM EDTA), placed in lysis solution, and electrophoresed in 1X TBE for 20 min at 1.5 V/cm. Micrographs were obtained using confocal microscopy (see below) which were subsequently analyzed using Comet IV software (Perceptive Instruments).

Terminal Deoxynucleotidyl Transferase Nick End Lableing (TUNEL) Assay

TUNEL assays were performed using an *in situ* cell death detection kit with FITC conjugated dUTP (Roche). Cells were grown on coverslips, fixed, and permeabilized according to manufacturer's recommendations. As recommended by the kit manufacturer, negative control coverslips were prepared without terminal deoxynucleotidyl transferase to determine background staining by FITC-dUTP solution. Positive control coverslips were treated with DNase I (3000 U/mL in 20 mM Tris-HCl, 1 mM $MgCl_2$, pH 7.5; Roche) for 15 min at room temperature after fixation. Coverslips were then incubated with terminal deoxynucleotidyl transferase and FITC-dUTPs for 1 hr at 37º, washed in PBS, and mounted using a Prolong Antifade kit (Invitrogen).

Confocal Fluorescence Microscopy

Micrographs were collected on a Zeiss LSM 510 confocal microscope. Data were collected at a resolution of 1024 x 1024 pixels using a 10X Plan Neofluar dry objective (NA = 0.30), 40X Plan-Neofluar oil immersion (NA = 1.3),

or 63X Plan-Apochromat oil immersion objective (NA = 1.4). Micrographs were processed using the Zeiss LSM Image Browser software.

Pulsed Field Gel Electrophoresis

BSC40 cells were trypsinized and washed 2X in cold PBS. Neocarzinostatin (Sigma) treatment of cells at 200 ng/mL for 1 hour was used to generate DNA breaks as a positive control. Cells were suspended at a concentration of 1 x 10^6 (~6.7 µg genomic DNA) cells per 100 µL of low melting agarose (Bio-Rad) and pipetted into disposable plug molds (Bio Rad). Plugs were placed in buffer containing 1% N-laurylsarcosine, 0.5 M ethylenediaminetetraacetic acid (EDTA), and 1 mg/mL proteinase K for 24 hr at 50˚C as recommended (26). Plugs were washed twice in 5 mL TE buffer (10 mM Tris, 1 mM EDTA), followed by an additional wash for 12 hours in 5 mL TE buffer at 4˚ with gentle agitation. Plugs were embedded in 1% PFGE grade agarose (Bio-Rad) and electrophoresed for 24 hr on a CHEF Mapper XA PFGE apparatus, kindly made available by the laboratory of Seth Bordenstein. Electrophoresis conditions used were previously described (24): 1) 6 V/cm for 24 hours, 120˚ occluded angle, 10-90 second switch times in 0.5X TBE buffer at 14˚C. 2)1.5 V/cm for 66 hours, 120˚ occluded angle, 50-5000s pulse times in 0.5X TBE buffer at 14˚C. After electrophoresis, the gel was stained with SYBR Gold (Invitrogen) diluted 1:10000 in 0.5x TBE for 12 hours. The fraction of DNA released from the plug (FR) was quantified using Bio-Rad Quantity One software. Because of the high sensitivity of SYBR Gold along with overloading the plugs,

significant background staining was observed. The amount of DNA per plug was lowered to the range of 200-500 ng, which reduced background, but still did not result in significantly different FR compared to the positive control. Molecular weight markers used in these experiments were H. wingei chromosomal DNA (Bio-Rad 170-3667), 0.05-1Mb λ ladder, (Bio-Rad 170-3635), and 8-48 kb ladder (Bio-Rad 170-3707). Data from these experiments are not shown.

Mitotracker Dyes

In order to detect mitochondrial ROS, Mitotracker Red CM-H_2XRos (Invitrogen), a probe that localizes in mitochondria and fluoresces only after mitochondrial membrane potential change. This was used in conjunction with Mitotracker Deep Red FM (Invitrogen), a general mitochondrial dye, was used in along with Mitotracker Red CM-H_2XRos to determine cellular location of mitochondria. Stock solutions of each Mitotracker probe were made at 1 mM in DMSO. Media was aspirated from cells and replaced with warm incomplete media containing 100 nM Mitotracker Red CM-H_2XRos and 50 nM Mitotracker Deep Red FM. Cells were incubated for 40 minutes at 37˚. After the incubation, cells were washed in cold PBS, fixed for 10 min in 4% paraformaldehyde in PBS, permeabilized for 2 min with 0.2% Triton X-100 in PBS, and washed three times in PBS. Nuclei were counterstained with 2.5 µg/mL 4’,6-diamidino-2-phenylindole (DAPI) in PBS. Coverslips were dried and mounted using Prolong Antifade Gold (Invitrogen). Antimycin A (Sigma) was used as a positive control for ROS generation. Stock solutions of antimycin A were prepared at 10 mg/mL

in 95% EtOH, diluted to 1 mM in dimethyl sulfoxide, and added to DMEM at a working concentration of 10 μM for 2-8 hours before Mitotracker treatment. Cells were visualized using confocal fluorescence microscopy. Although Mitotracker Deep Red FM labeling was successful under these conditions, Mitotracker Red CM-H_2XRos did not provide consistent results as fluorescence from this probe did not differ in untreated and antimycin A treated cells. Data from these experiments are not shown.

CHAPTER III

PRELIMINARY DATA

SV40 Induces Nuclear DNA Damage

Because of the established importance of DNA damage signaling during SV40 infection, members of the Fanning lab investigated whether this signaling was initiated by host DNA damage. TUNEL assays were used in a time course of SV40 infection to detect DNA breaks. Pan nuclear DNA damage in a significant fraction of the cells was first detected at 5 hpi (Fig. 3.1A), but appeared to decline at 20 hpi. A second time course of TUNEL assays was done to determine how long DNA damage persisted. While damage was still detected at 9 hpi, it appeared to decline 12-18 hpi (Fig. 3.1B). These data indicate that SV40 infection induces nuclear DNA breaks between 5 and 12 hpi.

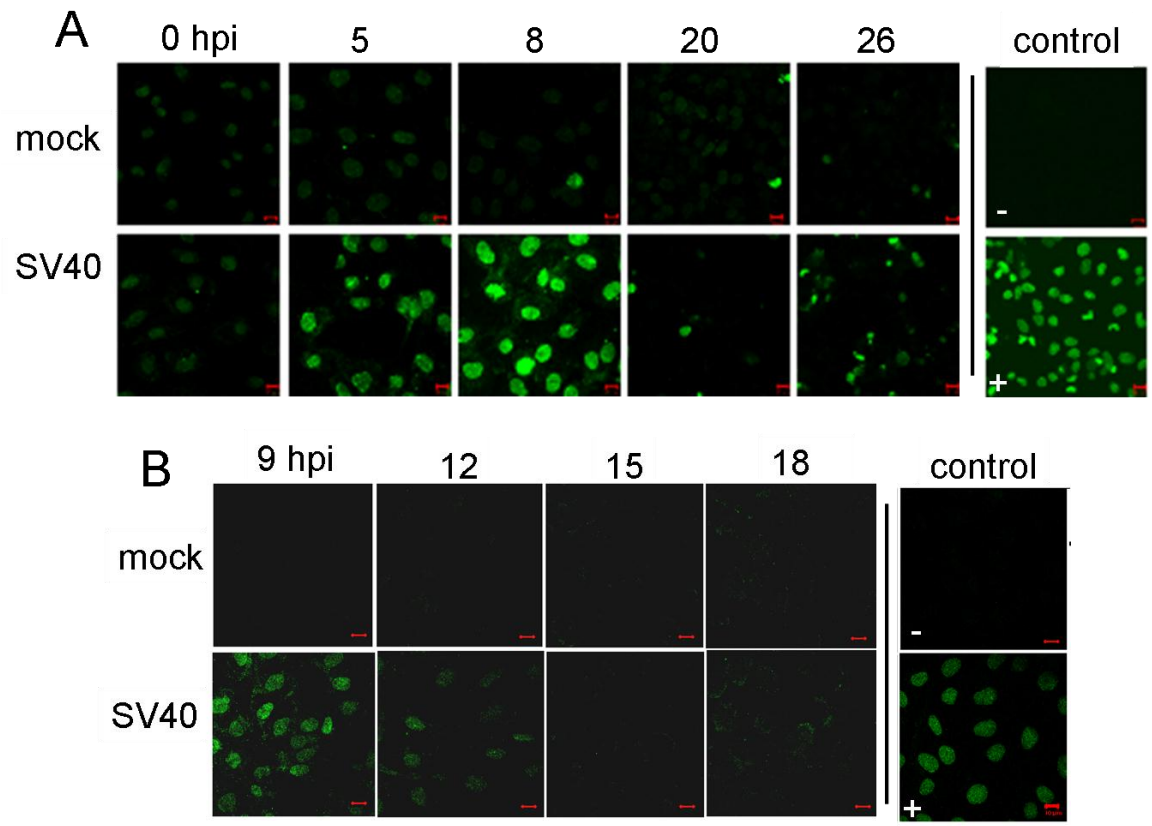

Figure 3.1. SV40 induces host nuclear DNA damage. A. BSC40 cells were infected with SV40 (MOI 10), fixed at the indicated time points, and probed for DNA breaks using a terminal deoxynucleotidyl transferase (Tdt) nick end labeling (TUNEL) kit. Negative control coverslips were treated with all reagents except Tdt. Positive control coverslips were treated with DNAse I after fixation. (Scale bar = 10 μm) **B.** A second TUNEL experiment was performed to assay DNA damage from 12-18 hpi as indicated. (Scale bar = 10 μm) *Data from X. Zhao and A. K. McCreless.*

N-acetyl-cysteine Reduces DNA Breaks

To confirm results obtained with TUNEL, a single cell gel electrophoresis (Comet) assay was used to quantify DNA breaks**.** Raw micrographs with 5-15 cells per image are shown in Fig. 3.2A and quantified in 3.2B. Quantifying percentage tail DNA, correlating with DNA breaks, that separated from the head

was done using Comet IV software. Consistent with the TUNEL assay, DNA damage was detected at 5 hpi by an increase in tail DNA in infected cells relative to mock infected cells (Fig. 3.2).

In order to determine if reactive oxygen species (ROS) might be responsible for SV40 induced DNA breaks, infected cells were treated with the antioxidant N-acetyl cysteine (NAC). SV40 infected cells that were treated with NAC displayed far less tail DNA by the Comet assay compared to untreated SV40 infected cells (Fig. 3.2B). These data suggest that host DNA damage is responsible for DNA damage signaling that arises during SV40 cell entry and that ROS may play a direct role in producing DNA lesions.

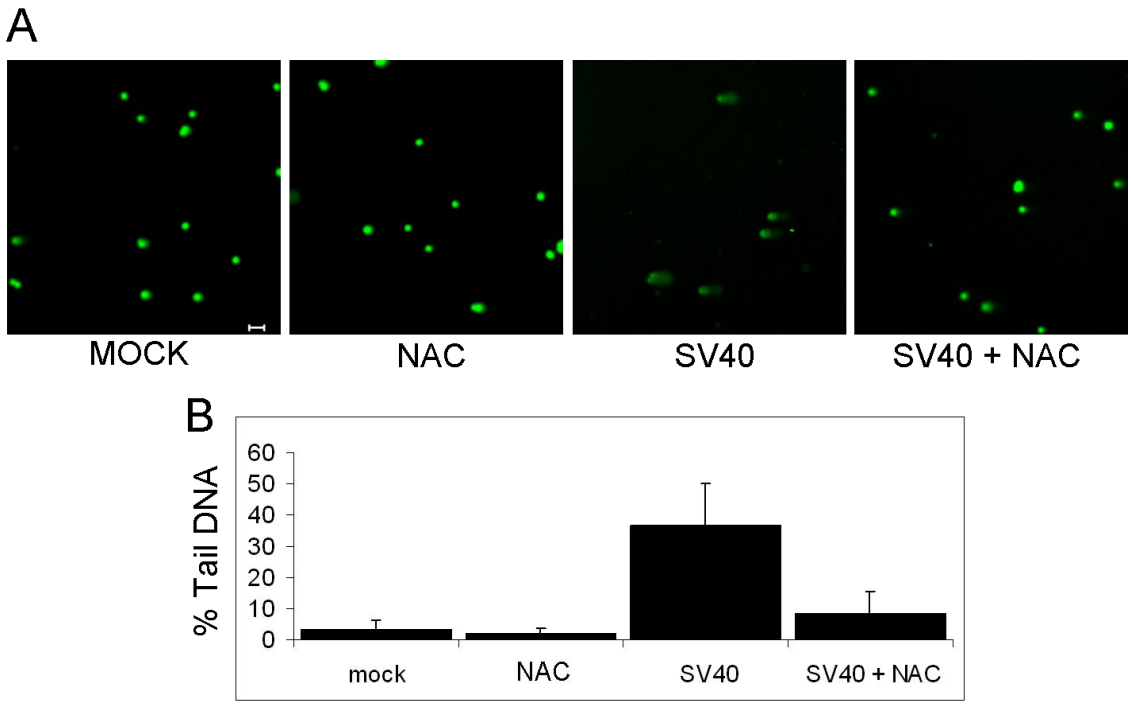

Figure 3.2. N-acetyl cysteine prevents SV40-induced DNA breaks. A. BSC40 cells, mock-infected or SV40-infected (MOI 10), were incubated from 2-5 hpi with or without 40 mM N-acetyl cysteine (NAC) as indicated. Whole cells were then examined in neutral comet assays. DNA electrophoresed out of the cells was

Figure 3. 2 continued. stained using SYBR Green (Scale bar = 50 μm) **B.** Percentage of tail DNA, a measure for DNA breaks, was quantified for 50 cells using Comet IV. Error bars indicate standard deviation. *Data from X. Zhao.*

Nocodazole and DTT Reduce SV40-induced DNA Breaks

In order to define better the events in SV40 entry that lead to host cell DNA breaks, small molecules were used to target specific steps of SV40 entry. SV40 containing vesicles budding from the caveosome require microtubules to move to the ER (60). This step was targeted with addition of nocodazole, which prevents microtubules polymerization, to SV40 infected cells to prevent the virus trafficking between the caveosome and the ER (60, 69). Using a TUNEL assay, it was found that nocodazole was able to prevent DNA breaks at 5 hpi (Fig. 3.3A).

From 4-8 hpi, SV40 uses host disulfide isomerases in the ER to rearrange capsid disulfide bonds that link adjacent VP1 molecules (43, 69). Dithiothreitol (DTT), a strong reducing agent, inhibits SV40 infection when added at 0 hpi, but has little effect on SV40 infection when added at 8 hpi (69). Generation of ROS from overuse of disulfide isomerases could be a genotoxic aspect of entry (85). Therefore, to determine whether inhibiting redox reactions with DTT would also inhibit DNA damage, a TUNEL assay on infected cells treated with DTT was performed. Again, DTT was able to reduce the DNA breaks as detected by TUNEL (Fig. 3.3B). Thus, creating a reducing cellular environment that has been demonstrated to inhibit disulfide oxidation and SV40 uncoating (60, 69), prevented induction of SV40-infection dependent DNA breaks.

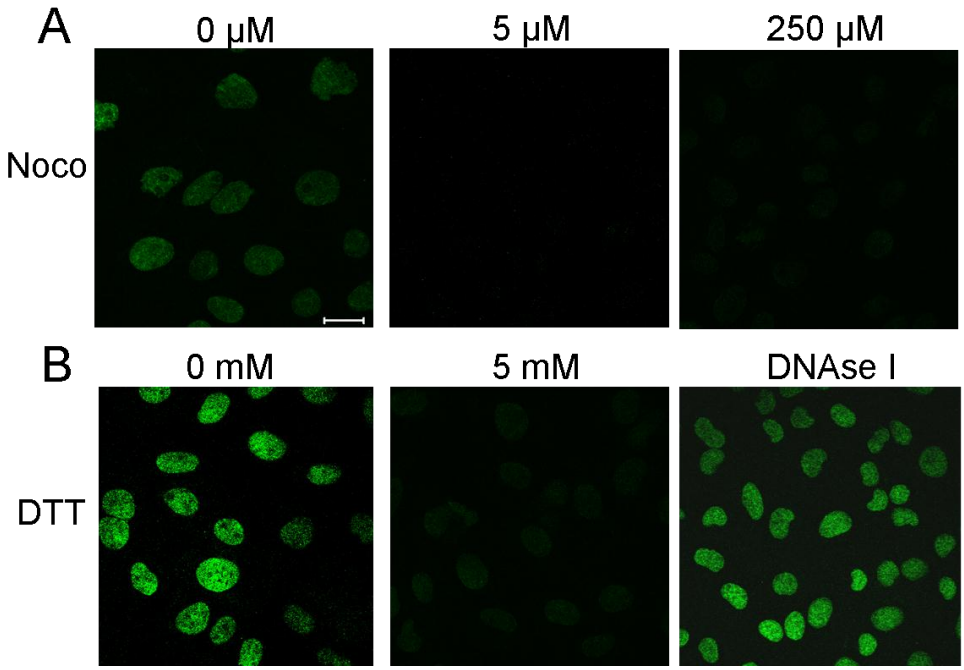

Figure 3.3. Transport of SV40 to the ER and redox are required for SV40 induced DNA breaks. BSC40 cells were infected at an MOI of 10. Either Nocodazole (**A**) or DTT (**B**) at the indicated concentration were added into cell culture medium at 2 hpi. Cels were fixed at 5 hpi, and a TUNEL assay was performed. (Scale bar = 20 μm) *Data from X. Zhao and B. Lou.*

CHAPTER IV

RESULTS

DNA Damage Signaling Arises before SV40 Early Gene Expression

In order to determine when DNA damage signaling first arises in SV40 infected cells, phosphorylation of histone H2AX (γH2AX) was assayed using indirect immunofluorescence through a time course of infection (Fig. 4.1). Neocarzinostatin (NCS), a radiomimetic drug that induces double strand DNA breaks, was used as a positive control to generate broken DNA, leading to γH2AX. Although an increase in γH2AX was clearly detected after Tag expression (Fig 4.1A, 15 hpi), some γH2AX foci could be detected at earlier times in uninfected cells. In order to carefully quantify the number of cells displaying γH2AX through SV40 infection, γH2AX positive cells were scored (Fig. 4.1C). The first increase in γH2AX was detected as early as 5 hpi and the number of positive cells increased through the infection time course. The earliest appearance of Tag was at 8 hpi (Fig. 4.1A), suggesting that DNA damage signaling began before production of early viral proteins.

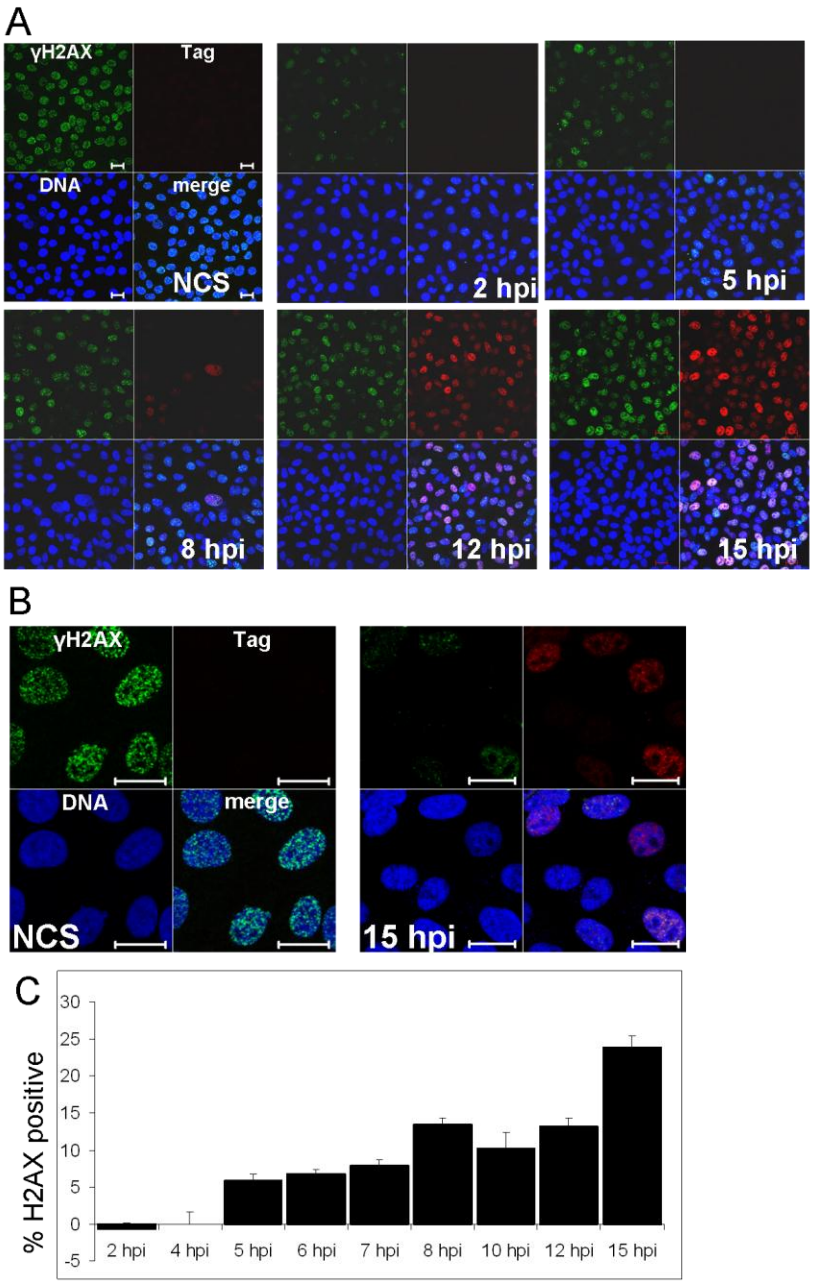

Figure 4.1. SV40 induces persistent γH2AX beginning at 5 hpi. A. BSC40 cells were infected with SV40 at MOI 10 or treated with neocarzinostatin. At the indicated times after infection, cells were pre-extracted, fixed, and immunofluorescently stained for γH2AX (green) and SV40 Tag (red). Nuclei were counterstained using TO-PRO-3 iodide (blue). Neocarzinostatin (NCS) served as a positive control for γH2AX staining. (Scale bar = 20 μm) **B.** High magnification examples of stained fields of cells (Scale bar = 20 μm) **C.** Five groups of 100 nuclei were scored for γH2AX at each time point. The average percentage of γH2AX-positive cells after subtraction of positive cells counted at 0 hpi is shown. Brackets indicate standard error of the mean.

Induction of γH2AX Is Dependent on Viral Multiplicity of Infection

The early appearance of γH2AX suggested that virus entry or uncoating might elicit DNA damage signaling. On the other hand, viral gene expression has been shown to induce damage signaling (8, 29). To test whether induction of γH2AX depends directly on SV40, BSC40 cells were infected at various multiplicities of infection (MOI). The number of infected cells was determined by Tag immunofluorescence at 24 hpi (Fig 4.2A). A greater percentage of cells express Tag with increasing viral multiplicity of infection. This result confirms that more cells are infected with an increasing MOI, as expected. To determine if the number of cells with activated DNA damage signaling also correlates with more infected cells, γH2AX immunofluorescence was performed at 8 hpi. The amount of γH2AX-positive cells increased with a higher MOI (Fig 4.2B). From micrographs in Fig. 4.2B, the number of γH2AX positive cells at each MOI were quantified. As with Tag, the percentage of γH2AX positive cells increased with MOI, suggesting a direct dependence between SV40 multiplicity of infection and DNA damage signaling.

UV Irradiated SV40 Induces γH2AX without Tag Expression

To investigate whether SV40 can induce DNA damage signaling in the absence of Tag expression, BSC40 cells were infected with UV-irradiated virus particles (UV-SV40). UV-SV40 did not express Tag detectable by Western blotting (Fig. 4.3A) or by immunofluorescence at 24 hpi (Fig. 4.3B). These results confirm that UV-SV40 was successfully inactivated. The level of UV-

SV40 induced γH2AX foci comparable to levels induced by mock irradiated virus (Fig. 4.3C).

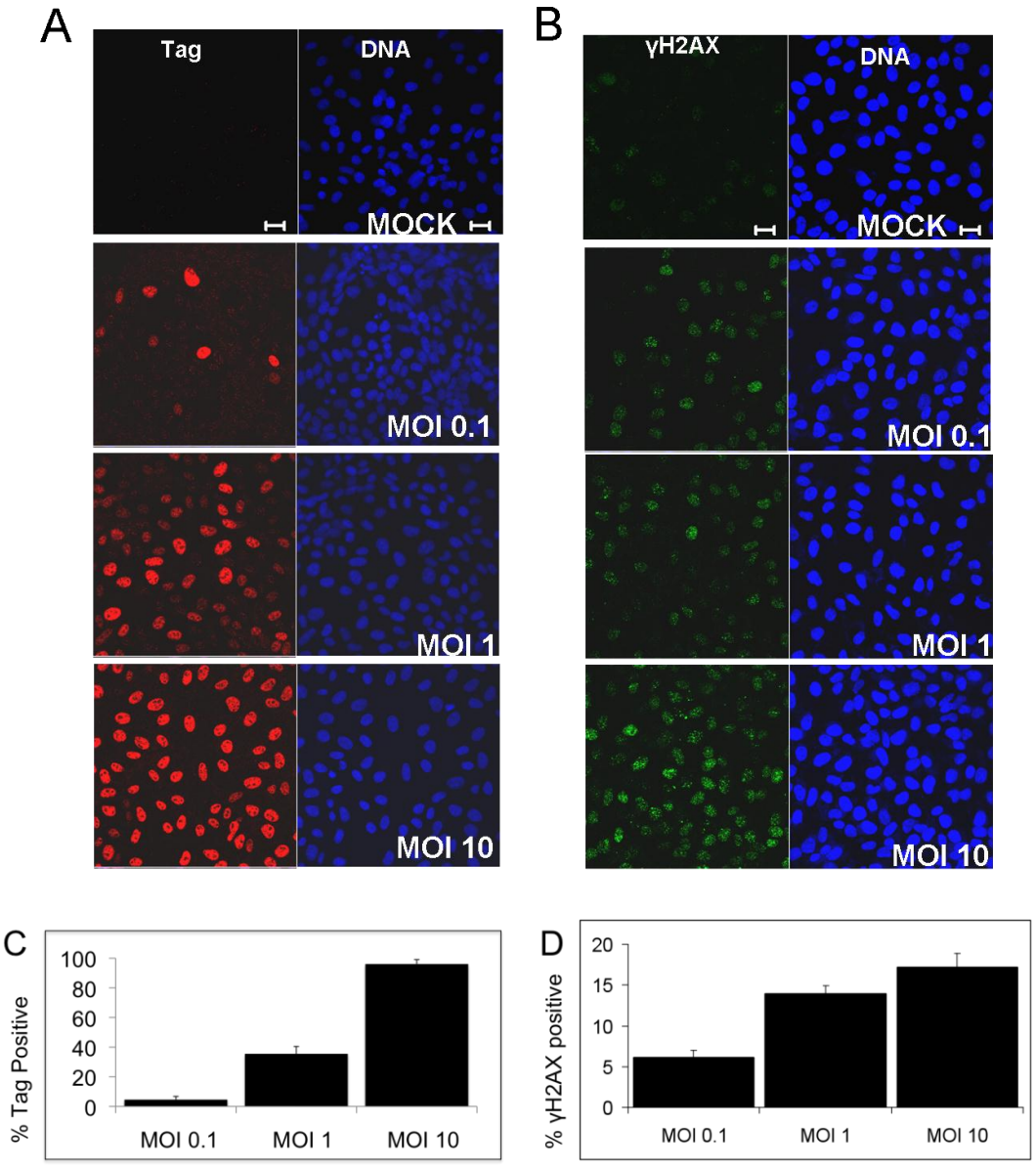

Figure 4.2. SV40-induced γH2AX is dependent on viral multiplicity of infection. In both A & B, BSC40 cells were infected with SV40 at varying multiplicities of infection. **A.** Cells were fixed at 24 hpi and Tag immunofluorescence (red) and TO-PRO-3 staining were performed. (Scale bar = 20 μm) **B.** Cells were fixed at 8 hpi and γH2AX immunofluorescence (green) was performed on BSC40 cells infected with SV40 at indicated MOI values. (Scale bar = 20 μm). Five groups of 100 nuclei were scored for Tag (**C**) or γH2AX (**D**) as in Figure 4.1C. Brackets indicate standard error of the mean.

Interestingly, γH2AX foci were not detected at 24 hpi in cells infected by UV-SV40 (Fig. 4.3B), suggesting that viral gene expression or other subsequent events in infected cells may be needed to maintain and potentiate DNA damage signaling. Taken together, these results argue that SV40 can induce DNA damage signaling as part of the cell entry process and in the absence of viral gene expression.

In order to confirm that DNA breaks are also an SV40 entry-mediated event, TUNEL assays were performed on cells infected with SV40 or UV-SV40 (Fig. 4.3D). Both viruses were able to induce comparable amounts of DNA damage at 5 hpi, indicating that DNA breaks at this point. These data provide evidence that DNA breaks and DNA damage signaling can occur independently of viral gene expression.

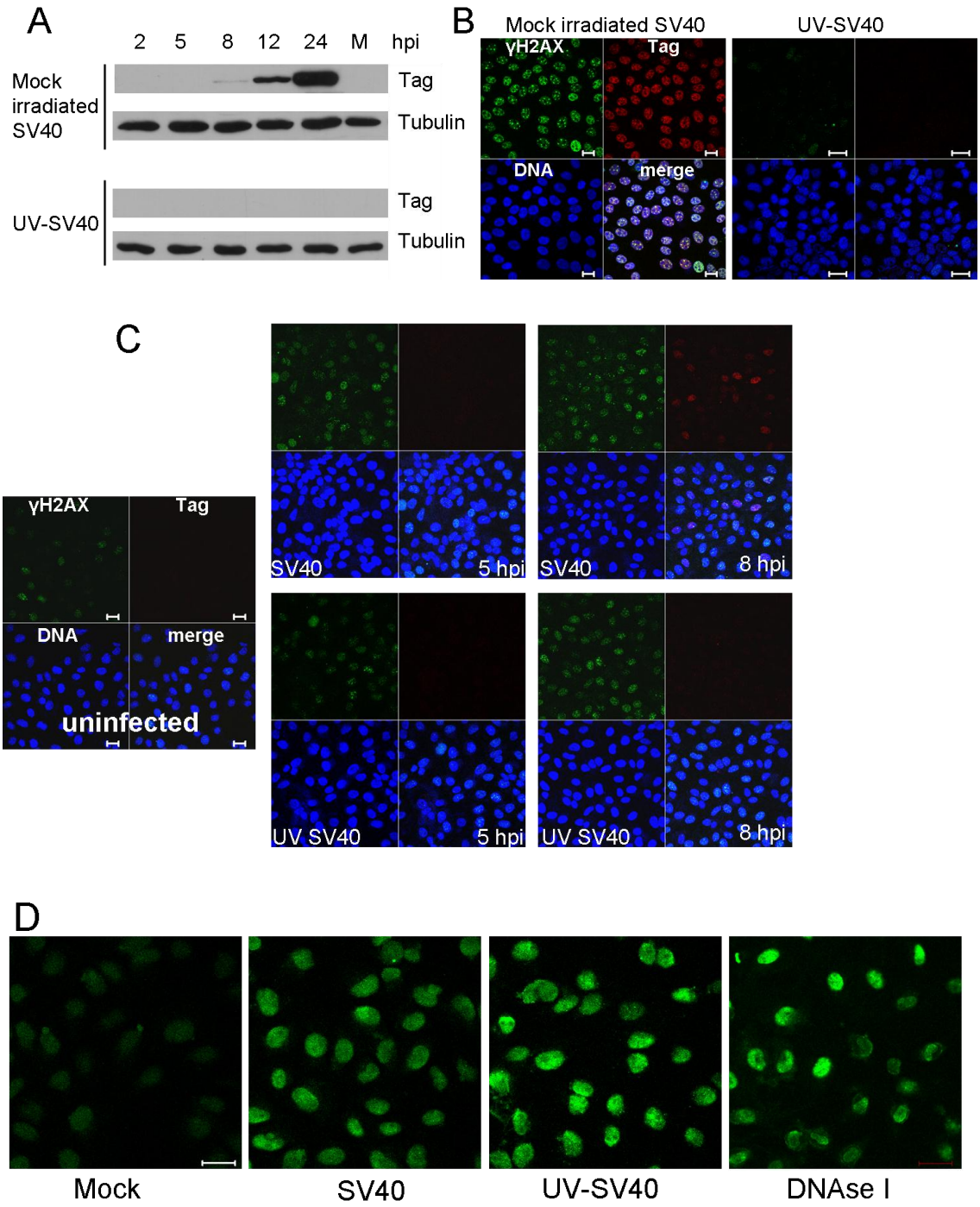

Figure 4.3. UV irradiated SV40 induces γH2AX. BSC40 cells were infected with either mock irradiated SV40 or SV40 that was UV irradiated for 5 minutes at MOI of 10. **A.** Western blots of whole cell extracts from SV40-infected BSC40 cells to detect viral protein expression. M, mock infected. B, C. Cells were pre-extracted, fixed, and stained for γH2AX (green) and Tag (red) at the indicated times after infection. (Scale bar = 20 μm) D. BSC40 cells were infected with SV40 or UV-SV40 (MOI 10), fixed at 5 hpi, and a TUNEL assay was performed.

The observation that N-acetyl-cysteine reduced SV40-induced DNA damage (Fig. 3.2) led us to investigate if this antioxidant was also able to reduce DNA damage signaling induced by SV40 infection (Fig. 4.1). First, the effect of NAC on γH2AX foci was tested by quantifying the fraction of γH2AX positive cells at 5 and 8 hpi (Fig. 4.4A). In the presence of 10 mM NAC, there was a significant reduction of γH2AX positive cells at 5 hpi and a slight reduction at 8 hpi (Fig. 4.4B). This result suggests that ROS may be involved in activating damage signaling before early gene expression. In order ask whether early gene expression also contributes to damage signaling, Tag and γH2AX immunofluorescence was performed again at 24 hpi (Fig. 4.4C and D). Comparing SV40-infected cells with NAC-treated infected cells, there was no difference in number of infected cells, indicating that NAC does not hinder SV40 infection (Fig. 4.4C). At 24 hpi, SV40 replication centers begin to form, which appear as large colocalized nuclear foci of Tag and γH2AX (80). NAC did not affect γH2AX foci formation or colocalization of Tag with γH2AX (Fig. 4.4D). This observation indicates that while ROS may be involved in generating DNA breaks during virus entry, other aspects of SV40 infection also contribute to DNA damage and/or DNA damage signaling later in infection.

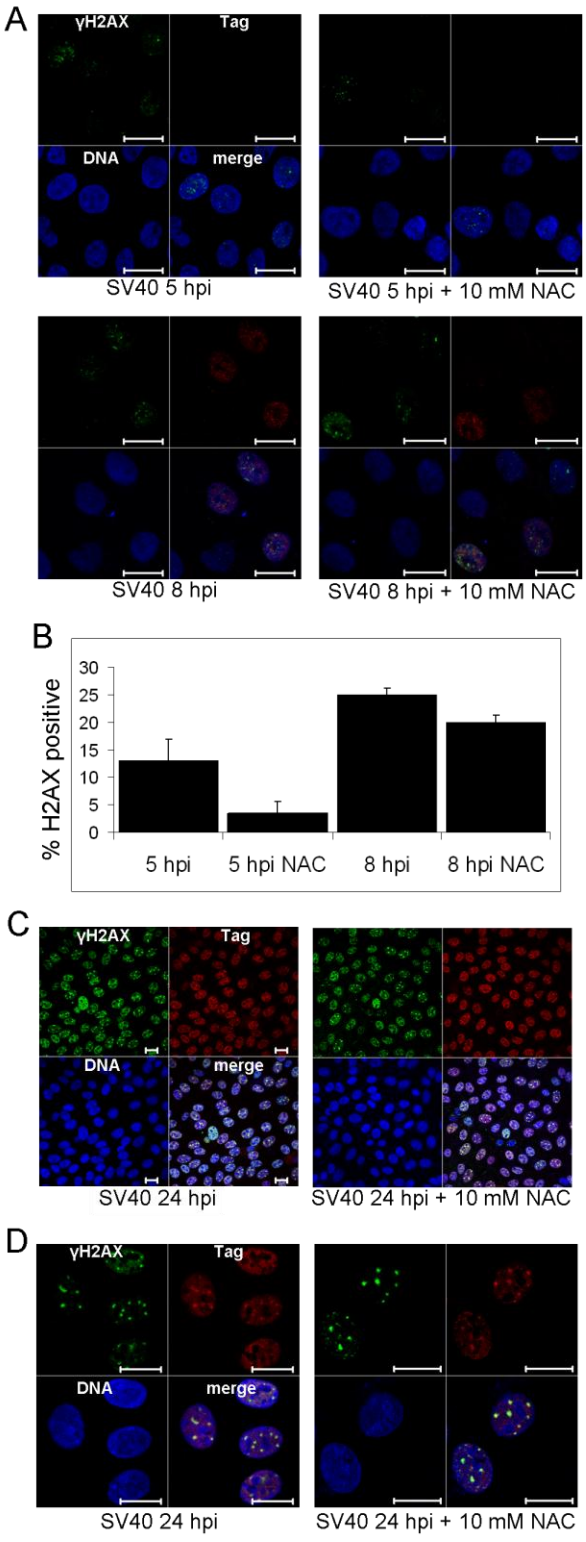

Figure 4.4. N-acetyl cysteine reduces γH2AX before, but not after early gene expression. BSC40 cells were infected with SV40 (MOI 10) with or without addition of 10 mM NAC at 2 hpi. **A.** At 5 or 8 hpi, cells were pre-extracted, fixed,

Figure 4.4, continued. and immunofluorescently stained for γH2AX (green) and SV40 Tag (red). Nuclei were counterstained using TO-PRO-3 iodide (blue). (Scale bar = 20 μm) **B.** Two groups of 100 cells were scored for γH2AX at the indicated time point. The number of positive cells in uninfected slides was subtracted. Brackets indicate standard error of the mean. **C.** At 24 hpi, cells were prepared as in A. (Scale bar = 20 μm) **D**. High magnification examples of cells from 4.4C (Scale bar = 20 μm).

SV40-induced DNA Breaks are Dependent on Calcium

Because preliminary evidence suggested that SV40 trafficked to the ER may induce host DNA breaks and that ROS may be produced at this time, we hypothesized that ER stress may contribute to DNA breaks. A similar pattern of entry events is seen with Hepatitis C Virus (77). ROS production in this pathway is dependent on Ca^{+2} leaking out of the ER into mitochondria at mitochondrial-ER interfaces (73). In order to test the hypothesis that Ca^{+2} leakage from the ER may induce ROS in SV40 infection, the effects BAPTA-AM, a calcium chelator, and Ru-360, an inhibitor of mitochondrial Ca^{+2} uptake, were added to SV40-infected cells and DNA breaks were assessed using a TUNEL assay (Fig. 4.5). SV40 infected cells treated with either BAPTA-AM or Ru-360 displayed fewer DNA breaks than untreated infected cells. These preliminary data indicate that calcium mobilization is important for SV40-induced DNA breaks.

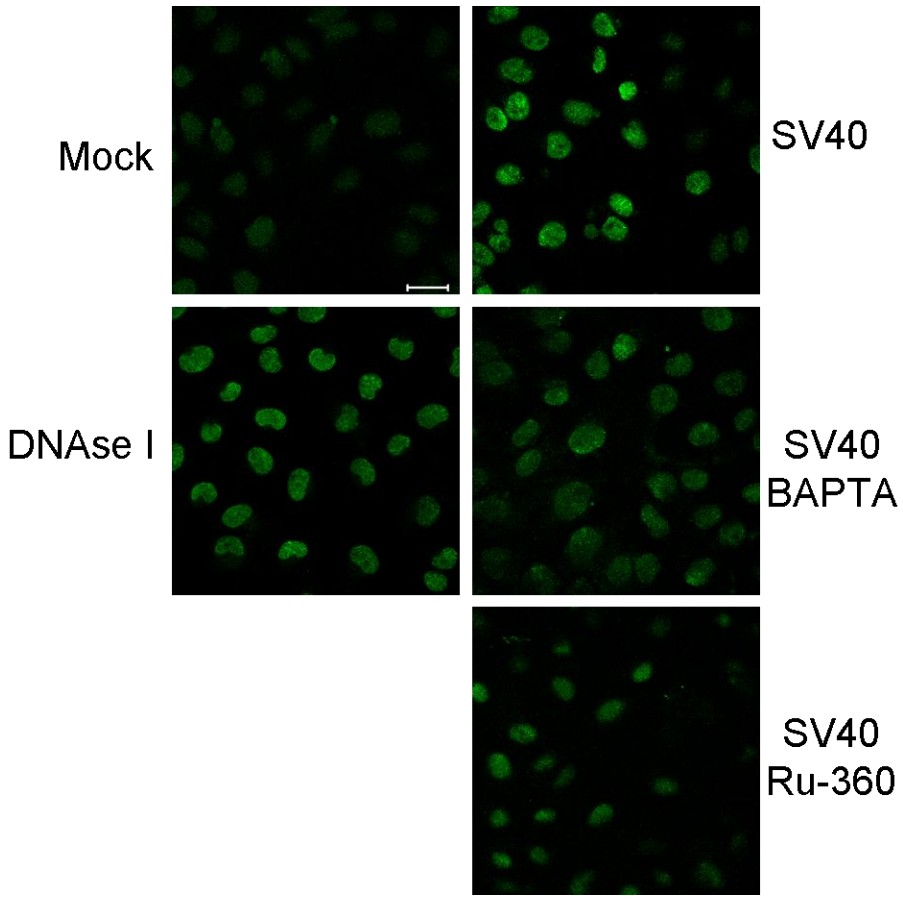

Figure 4.5. Cytoplasmic calcium influences SV40-induced DNA damage. BSC40 cells were infected at an MOI of 10. BAPTA-AM (100 μM) or Ru-360 (100 nm) were added at 2 hpi. Cells were fixed at 5 hpi, and a TUNEL assay was performed. (Scale bar = 20 μm)

SV40 Causes IκB-α Degradation

Oxidative stress and changes in cellular calcium concentration due to ER stress could cause activation of NF-κB signaling (70, 71). Activation of the NF-κB pathway leads to phosphorylation of the IκB, allowing NF-κB to move into the nucleus and activate transcription of target genes. (27). In order to determine if SV40 activates NF-κB signaling, the level of IκB-α was measured during a time

course of SV40 infection (Fig. 4.6). Thapsigargin, a small molecule that prevents a Ca^{+2} pump from concentrating calcium in the ER, was used as a positive control that triggers IκB-α degradation. At MOI 1, a modest decrease in IκB-α was observed after virus uptake (2 hpi; Fig. 4.6A). Then, the level of IκB-α recovered to near mock levels and stayed constant 5-12 hpi. At 12-24 hpi, a drop was again observed. At MOI 10, there is a similar drop in IκB-α at 2 hpi, but did not recover to mock levels (Fig. 4.6B). Similar to MOI 1, there is a noticeable drop at 24 hpi relative to 12 hpi. SV40-induced ER stress leading to IκB degradation may be reflected in the drop of between 5 and 8 hpi. in Fig. 4.6B. The drop in IκB at 2 hpi likely indicates other signaling associated with entry (10). The ATM-mediated DNA damage response is also a candidate to activate NF-κB throughout SV40 infection (83).

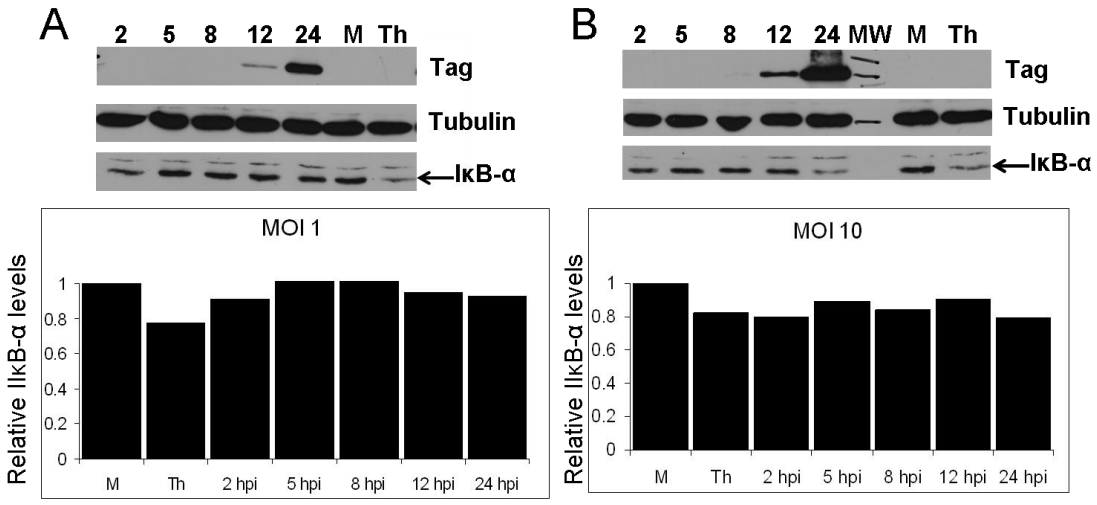

Figure 4.6. SV40 induces IκB degradation. BSC40 cells were infected with SV40 (MOI 1 or 10), mock infected, or treated with thapsigargin as a positive control. Western blots of whole cell extracts from cells were probed for Tag as a marker for SV40 infection, tubulin as a loading control, and IκB-α. M, mock infected (24 hr). Th, 2 μM Thapsigargin for 12 hr. Blots and quantifications for a

time course of SV40 infection at **A.** MOI 1 and **B.** MOI 10 are shown. Quantification of IκB-α levels normalized to tubulin with mock infected set as 1.

SV40-induced DNA Breaks Do Not Occur in Non-permissive Cells

In order to investigate if SV40 uptake alone is sufficient to produce DNA damage, or if the DNA breaks result from a more complex interaction between SV40 and the host cell, NIH3T3 mouse cells were infected with SV40 and DNA breaks were detected with a TUNEL assay. SV40 is not able to replicate in 3T3 cells. Although pan nuclear γH2AX and Tag were found in nuclei of infected 3T3 cells after 24 hpi, no organization of SV40 replication centers was observed (86). Surveying a time course of SV40 infection from 5 to 24 hours, no DNA breaks were detected by TUNEL (Fig. 4.7). This result indicates that DNA damage that occurs as part of cell entry may be important for orchestrating the DNA damage response to facilitate viral DNA replication.

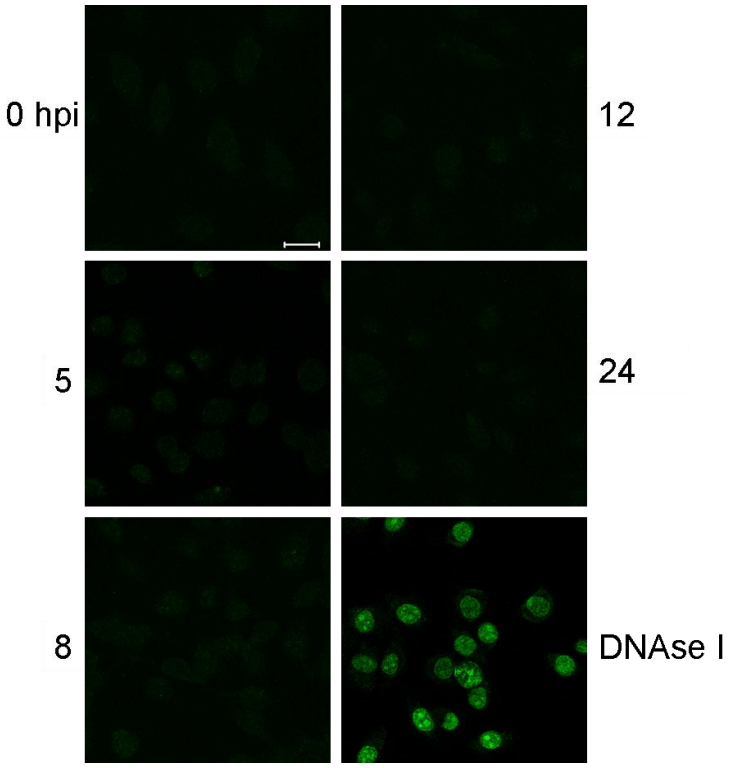

Figure 4.7. SV40 does not induce DNA breaks in non-permissive mouse cells. **A.** NIH-3T3 cells were infected with SV40 (MOI of 10), fixed, and a TUNEL assay was performed at the indicated time points. (Scale bar = 20 μm)

CHAPTER V

DISCUSSION

Summary of Results and Model

Here we present a novel mechanism of DNA damage associated with entry of a nonenveloped virus. This mechanism is supported by the observation that DNA damage (Fig. 3.1) and γH2AX (Fig. 4.1) arise at 5 hpi, before Tag is detected (Fig. 4.3). Further, UV inactivated SV40 that cannot express Tag still generates DNA breaks and γH2AX positive cells at levels comparable to those observed in mock-irradiated SV40-infected cells (Fig. 4.3).

A hypothetical model for how SV40 induces DNA damage during cell entry is summarized in Fig. 5.1. As incoming SV40 accumulates in the ER between 4-6 hpi (34, 60), redox enzymes that form and break disulfide bonds act on VP1 in the SV40 capsid. Disulfide bonds that began as intermolecular linkages between VP1 molecules change to intramolecular VP1 bonds (69). This process generates ROS as O_2 acts as a reserve electron acceptor. In the presence of ROS, calcium is released from the ER, and induces mitochondrial ROS release, (85) eventually leading to DNA damage.

Both the c-Jun N-terminal kinase (JNK) and mitogen activated protein kinase (MAPK) pathways are activated during ER stress (66). The importance of JNK or MAPK signaling during SV40 infection has not been tested. Determining the effect of small molecule inhibitors of JNK (7) and p38-MAPK (13) could be

used to address the importance of these kinases during SV40 infection. Another possibility is that ROS directly activates DNA damage signaling through ATM (26).

SV40 Activates the DNA Damage Response in Multiple Ways

Even though SV40 or JCV Tag protein expression alone causes DNA breaks and DNA damage signaling in human cells in the absence of viral infection (8, 29, 57), our results indicate an additional mechanism that SV40 uses to initiate DNA damage signaling. SV40 Tag expression is proposed to cause DNA breaks and activate the DNA damage response through an interaction with the spindle checkpoint protein Bub1 (8, 29). However, the contribution of the Tag-Bub1 interaction to host DNA damage during SV40 infection has not been addressed.

Another mechanism proposed to be important for Tag-induced DNA breaks is the ability of Tag to bind host chromatin (57). But, again, testing the effect of making corresponding mutations proposed to disrupt such nonspecific DNA interactions (45, 82) on host genotoxicity has not been done in the context of viral infection. Further, the effect of these mutations on other interactions of Tag with host proteins has not been assessed. It is possible that the complex signaling that occurs during polyomavirus infection results in post-translational modification of viral (72) and host proteins (64) that modulates their activities, resulting in host effects that vary drastically from ectopic expression of a viral protein.

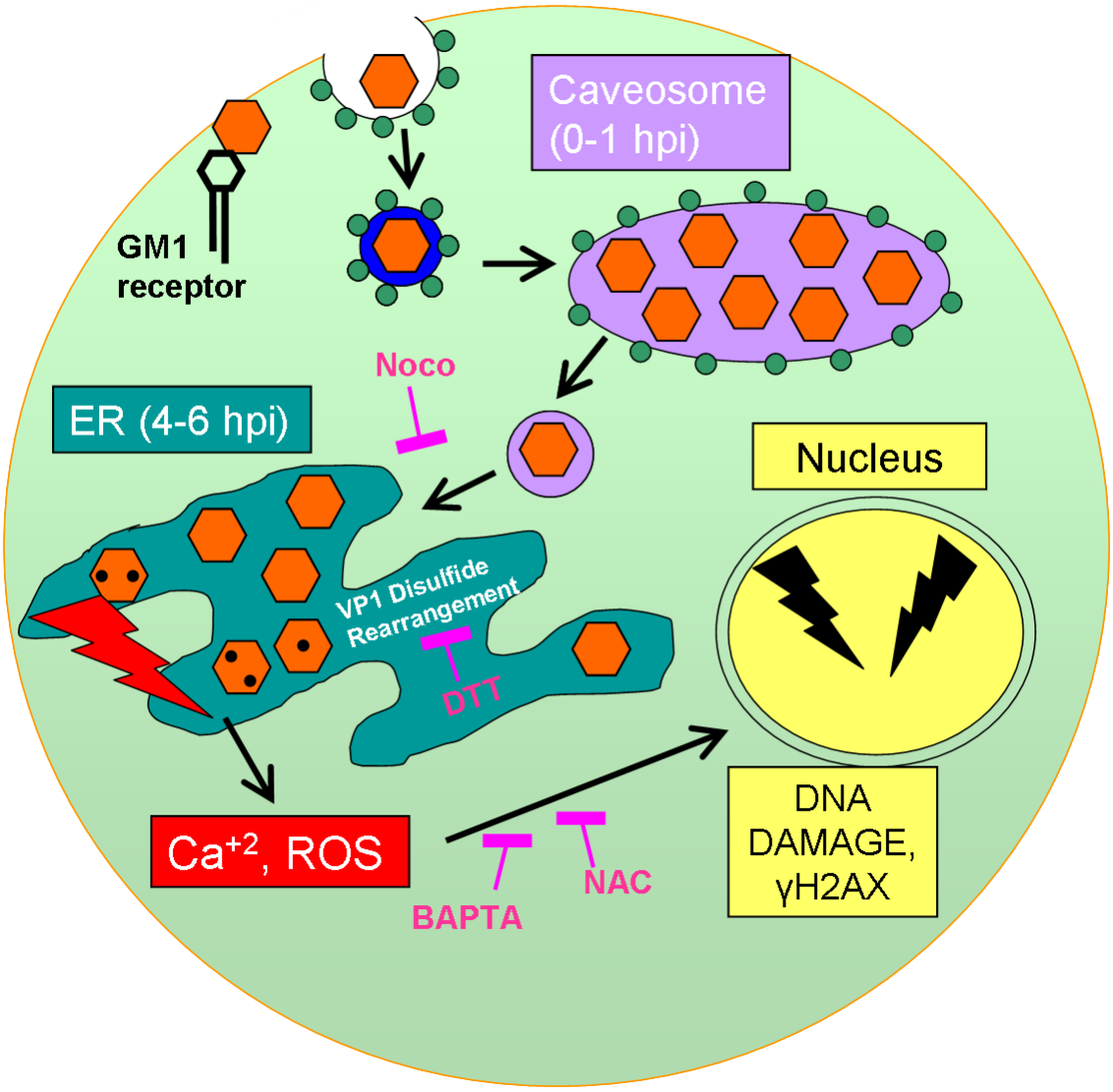

Figure 5.1. Model for host genotoxicity generated by SV40 entry. See text for details.

Maintenance of DNA Damage Signaling

An intriguing aspect of the data presented here is that host DNA breaks disappeared at 12 hpi (Fig. 3.1), but γH2AX continued to increase through 15 hpi

(Fig. 4.1). At 24 hpi, γH2AX was not found in cells infected with UV-SV40 (Fig. 4.3B). These results imply that viral gene expression is required to maintain DNA damage signaling. For example, small t-antigen binds and inhibits protein phosphatase 2A (PP2A) activity (59, 68). PP2A has been shown to colocalize with γH2AX foci and promote dephosphorylation of γH2AX to facilitate DNA break repair (11).

Another mechanism that SV40 could use to prolong the DNA damage response is preventing dephosphorylation of DNA damage response substrates through interaction of Tag with phospho-proteins. Tag is proposed to have a single breast cancer tumor suppressor C-terminus (BRCT) domain based on structural and sequence data (37). These domains generally bind to phosphoproteins (84). The hexameric state of Tag would provide the basis of positioning two BRCT domains side by side, as many BRCT domains often appear in pairs in proteins. However, the description of a BRCT domain in Tag remains lacks corroborating biological evidence showing that Tag uses this domain to interact with specific cellular phosphoproteins.

Virus Interactions with Ca^{+2} and ROS

The potential roles of ROS during SV40 entry

Our observation that NAC inhibited DNA breaks and DNA damage signaling at 5 hpi suggests that oxidative events early in infection, e.g. ROS, play a role in generating host DNA damage. The fact that NAC does not completely

abrogate SV40-induced γH2AX indicates that SV40 has multiple ways of initiating DNA damage signaling. If the model is correct, we expect to detect these cellular ROS around 5 hpi, concurrent with γH2AX (Fig. 4.1) and DNA damage (Fig. 3.1).

However, because NAC protects against SV40-induced DNA breaks (Fig 3.2) and does not negatively affect SV40 infection or organization of viral replication centers (Fig. 4.4), perhaps ROS are not a critical aspect of SV40 infection in cell culture. If cellular ROS production is a side effect of SV40 entry not essential for infection, treatment of infected cells could help viral DNA replication by preventing lesions in viral DNA introduced by ROS. It is counterintuitive that SV40 may create an oxidative host environment concurrent with the release of its own genome, possibly causing lesions in viral DNA. Perhaps the oxidation enables H2AX packaged with the SV40 minichromosome to become phosphorylated and recruit damage response proteins to sites of viral DNA replication (86).

Generating ER stress during SV40 entry

SV40 can enter by caveolin-mediated or caveolin-independent endocytosis (50). In both cases, the GM1 ganglioside is the preferred receptor for SV40 (78). Since GM1 accumulates at the ER at areas of interaction with mitochondria, it can perturb Ca^{+2} homeostasis, promoting ER stress and apoptosis (67). The release of calcium into the cytoplasm could be influenced by accumulation of the GM1 ganglioside that enters as part of viral endocytosis and

accumulates in the ER. However, because the ganglioside used by different polyomaviruses varies (19, 46, 78), this potential mechanism may be unique for SV40. In a novel mechanism, JCV agnoprotein has recently been shown to localize to the ER and promote movement of Ca^{+2} into the cytoplasm (76). An analogous function of SV40 agnoprotein has not been investigated. Because agnoprotein is expressed from a late promoter and is not packaged with the capsid, it is not likely involved in entry ER permeabilization, but could be involved in changing Ca^{+2} homeostasis in a later phase of infection.

The requirement of retrotranslocation from ER to cytoplasm for SV40 entry suggests that ER stress activates the ERAD pathway during SV40 entry. ER stress can be activated when Ire1, a central ER sensor of protein folding, oligomerizes due to multiple contacts with unfolded proteins (41). It is interesting to consider that SV40 within the ER could artificially stimulate such Ire1 mediated stress signaling. In this model, VP1 would interact directly with Ire1 to create oligomers and stimulate the unfolded protein response.

The truly important effects of cellular entry could come from inducing host cell stress through the unfolded protein response. Such cellular stress could contribute to activation of caspases that are essential for infection (10). The substrates cleaved by caspases that facilitate SV40 infection have not yet been defined. The contribution of caspases to nuclear DNA fragmentation has not been addressed. Considering the low levels of caspase activation during entry and the fact that the SV40 lytic cycle lasts over 3 days, it is unlikely that apoptotic signaling advances far enough to stimulate the caspase activated DNase (CAD).

Further, general nuclease activity of CAD would also degrade the viral genome. Determining if SV40 causes DNA breaks in the presence of a pan-caspase inhibitor (Z-VAD-FMK) could help resolve this question.

Interactions of other viruses with ROS

ROS play an important role during other viral interactions with host cells. Hepatitis C virus (HCV) has multiple documented mechanisms for generating oxidative stress. NS5A disrupts ER Ca^{+2} leading to ROS production and resulting in stimulation of NF-KB signaling (24). A later study showed that HCV core, E1, and NS3 each contribute to production of cellular ROS (48). Along with ROS, induction of nitric oxide synthase leads to DNA damage (48, 49). The HCV core protein localizes to mitochondria and stimulates mitochondrial calcium uptake (42). In addition, HCV induces overexpression of an NADPH oxidase 4 that contributes to ROS (9). In a similar manner, Epstein-Barr virus (EBV) EBNA-1 protein creates ROS and DNA breaks by inducing NADPH oxidase 2 transcription. Like Tag, EBNA-1 is a DNA binding protein (39), but the requirement of this function in host genotoxicity has not been investigated. ROS and genome instability are likely important in HCV and EBV tumorigenesis and could also be an important aspect of polyomavirus biology.

Which Host Cell Effects Are Essential for SV40 Infection?

The observation that SV40 does not cause DNA breaks in one non-permissive mouse cell line (Fig. 4.7), but is still able to uncoat, express early

genes, and generate γH2AX, may be a clue that entry mediated DNA damage is important for preparing the host cell to facilitate viral DNA replication. A broader generalization could be made that the organism or tissue accounts for this difference. An additional argument is that DNA breaks that occur due to SV40 infection of BSC40 cells is a unique effect observed in a specific cultured cell line. For example, DNA breaks were not observed during SV40 infections of CV-1 cells (10).

The novel aspect of SV40 entry presented here is that host DNA breaks occur and the DNA damage response is activated independently of viral gene expression. However, direct evidence that SV40 induces ER stress, causes host oxidative stress, or causes Ca^{+2} to leave the ER is lacking. Carefully determining the interactions of cellular components with virus entry and ascertaining the effects they have on the processes of viral entry, gene expression, viral DNA replication, and assembly will be important for a comprehensive understanding of SV40 biology.

REFERENCES

1. **Adeyemi, R. O., S. Landry, M. E. Davis, M. D. Weitzman, and D. J. Pintel.** 2010. Parvovirus minute virus of mice induces a DNA damage response that facilitates viral replication. PLoS Pathog **6**.
2. **Ahuja, D., M. T. Saenz-Robles, and J. M. Pipas.** 2005. SV40 large T antigen targets multiple cellular pathways to elicit cellular transformation. Oncogene **24:**7729-45.
3. **Allander, T., K. Andreasson, S. Gupta, A. Bjerkner, G. Bogdanovic, M. A. Persson, T. Dalianis, T. Ramqvist, and B. Andersson.** 2007. Identification of a third human polyomavirus. J Virol **81:**4130-6.
4. **Arroyo, J. D., and W. C. Hahn.** 2005. Involvement of PP2A in viral and cellular transformation. Oncogene **24:**7746-55.
5. **Baker, T. S., J. Drak, and M. Bina.** 1989. The capsid of small papova viruses contains 72 pentameric capsomeres: direct evidence from cryo-electron-microscopy of simian virus 40. Biophys J **55:**243-53.
6. **Baker, T. S., J. Drak, and M. Bina.** 1988. Reconstruction of the three-dimensional structure of simian virus 40 and visualization of the chromatin core. Proc Natl Acad Sci U S A **85:**422-6.
7. **Bennett, B. L., D. T. Sasaki, B. W. Murray, E. C. O'Leary, S. T. Sakata, W. Xu, J. C. Leisten, A. Motiwala, S. Pierce, Y. Satoh, S. S. Bhagwat, A. M. Manning, and D. W. Anderson.** 2001. SP600125, an anthrapyrazolone inhibitor of Jun N-terminal kinase. Proc Natl Acad Sci U S A **98:**13681-6.
8. **Boichuk, S., L. Hu, J. Hein, and O. V. Gjoerup.** 2010. Multiple DNA damage signaling and repair pathways deregulated by simian virus 40 large T antigen. J Virol **84:**8007-20.
9. **Boudreau, H. E., S. U. Emerson, A. Korzeniowska, M. A. Jendrysik, and T. L. Leto.** 2009. Hepatitis C virus (HCV) proteins induce NADPH oxidase 4 expression in a transforming growth factor beta-dependent manner: a new contributor to HCV-induced oxidative stress. J Virol **83:**12934-46.
10. **Butin-Israeli, V., N. Drayman, and A. Oppenheim.** 2010. Simian virus 40 infection triggers a balanced network that includes apoptotic, survival, and stress pathways. J Virol **84:**3431-42.
11. **Chowdhury, D., M. C. Keogh, H. Ishii, C. L. Peterson, S. Buratowski, and J. Lieberman.** 2005. gamma-H2AX dephosphorylation by protein phosphatase 2A facilitates DNA double-strand break repair. Mol Cell **20:**801-9.
12. **Cimprich, K. A., and D. Cortez.** 2008. ATR: an essential regulator of genome integrity. Nat Rev Mol Cell Biol **9:**616-27.
13. **Cuenda, A., J. Rouse, Y. N. Doza, R. Meier, P. Cohen, T. F. Gallagher, P. R. Young, and J. C. Lee.** 1995. SB 203580 is a specific inhibitor of a

MAP kinase homologue which is stimulated by cellular stresses and interleukin-1. FEBS Lett **364:**229-33.

14. **Dahl, J., J. You, and T. L. Benjamin.** 2005. Induction and utilization of an ATM signaling pathway by polyomavirus. J Virol **79:**13007-17.
15. **Dalianis, T., T. Ramqvist, K. Andreasson, J. M. Kean, and R. L. Garcea.** 2009. KI, WU and Merkel cell polyomaviruses: a new era for human polyomavirus research. Semin Cancer Biol **19:**270-5.
16. **Damm, E. M., L. Pelkmans, J. Kartenbeck, A. Mezzacasa, T. Kurzchalia, and A. Helenius.** 2005. Clathrin- and caveolin-1-independent endocytosis: entry of simian virus 40 into cells devoid of caveolae. J Cell Biol **168:**477-88.
17. **Daniels, R., N. M. Rusan, P. Wadsworth, and D. N. Hebert.** 2006. SV40 VP2 and VP3 insertion into ER membranes is controlled by the capsid protein VP1: implications for DNA translocation out of the ER. Mol Cell **24:**955-66.
18. **Dunn, S. D.** 1986. Effects of the modification of transfer buffer composition and the renaturation of proteins in gels on the recognition of proteins on Western blots by monoclonal antibodies. Anal Biochem **157:**144-53.
19. **Erickson, K. D., R. L. Garcea, and B. Tsai.** 2009. Ganglioside GT1b is a putative host cell receptor for the Merkel cell polyomavirus. J Virol **83:**10275-9.
20. **Fanning, E., and K. Zhao.** 2009. SV40 DNA replication: from the A gene to a nanomachine. Virology **384:**352-9.
21. **Feng, H., M. Shuda, Y. Chang, and P. S. Moore.** 2008. Clonal integration of a polyomavirus in human Merkel cell carcinoma. Science **319:**1096-100.
22. **Gardner, S. D., A. M. Field, D. V. Coleman, and B. Hulme.** 1971. New human papovavirus (B.K.) isolated from urine after renal transplantation. Lancet **1:**1253-7.
23. **Gaynor, A. M., M. D. Nissen, D. M. Whiley, I. M. Mackay, S. B. Lambert, G. Wu, D. C. Brennan, G. A. Storch, T. P. Sloots, and D. Wang.** 2007. Identification of a novel polyomavirus from patients with acute respiratory tract infections. PLoS Pathog **3:**e64.
24. **Gong, G., G. Waris, R. Tanveer, and A. Siddiqui.** 2001. Human hepatitis C virus NS5A protein alters intracellular calcium levels, induces oxidative stress, and activates STAT-3 and NF-kappa B. Proc Natl Acad Sci U S A **98:**9599-604.
25. **Gruhne, B., R. Sompallae, D. Marescotti, S. A. Kamranvar, S. Gastaldello, and M. G. Masucci.** 2009. The Epstein-Barr virus nuclear antigen-1 promotes genomic instability via induction of reactive oxygen species. Proc Natl Acad Sci U S A **106:**2313-8.
26. **Guo, Z., S. Kozlov, M. F. Lavin, M. D. Person, and T. T. Paull.** 2010. ATM activation by oxidative stress. Science **330:**517-21.
27. **Hayden, M. S., and S. Ghosh.** 2008. Shared principles in NF-kappaB signaling. Cell **132:**344-62.

28. **Heacock, M. L., D. F. Stefanick, J. K. Horton, and S. H. Wilson.** 2010. Alkylation DNA damage in combination with PARP inhibition results in formation of S-phase-dependent double-strand breaks. DNA Repair (Amst) **9:**929-36.
29. **Hein, J., S. Boichuk, J. Wu, Y. Cheng, R. Freire, P. S. Jat, T. M. Roberts, and O. V. Gjoerup.** 2009. Simian virus 40 large T antigen disrupts genome integrity and activates a DNA damage response via Bub1 binding. J Virol **83:**117-27.
30. **Herschleb, J., G. Ananiev, and D. C. Schwartz.** 2007. Pulsed-field gel electrophoresis. Nat Protoc **2:**677-84.
31. **Hill, R., and P. W. Lee.** 2010. The DNA-dependent protein kinase (DNA-PK): More than just a case of making ends meet? Cell Cycle **9:**3460-9.
32. **Jackson, S. P., and J. Bartek.** 2009. The DNA-damage response in human biology and disease. Nature **461:**1071-8.
33. **Jiang, M., J. R. Abend, B. Tsai, and M. J. Imperiale.** 2009. Early events during BK virus entry and disassembly. J Virol **83:**1350-8.
34. **Kartenbeck, J., H. Stukenbrok, and A. Helenius.** 1989. Endocytosis of simian virus 40 into the endoplasmic reticulum. J Cell Biol **109:**2721-9.
35. **Kean, J. M., S. Rao, M. Wang, and R. L. Garcea.** 2009. Seroepidemiology of human polyomaviruses. PLoS Pathog **5:**e1000363.
36. **Khalili, K., M. K. White, H. Sawa, K. Nagashima, and M. Safak.** 2005. The agnoprotein of polyomaviruses: a multifunctional auxiliary protein. J Cell Physiol **204:**1-7.
37. **Kumar, A., W. S. Joo, G. Meinke, S. Moine, E. N. Naumova, and P. A. Bullock.** 2008. Evidence for a structural relationship between BRCT domains and the helicase domains of the replication initiators encoded by the Polyomaviridae and Papillomaviridae families of DNA tumor viruses. J Virol **82:**8849-62.
38. **Lavin, M. F., and S. Kozlov.** 2007. ATM activation and DNA damage response. Cell Cycle **6:**931-42.
39. **Leight, E. R., and B. Sugden.** 2000. EBNA-1: a protein pivotal to latent infection by Epstein-Barr virus. Rev Med Virol **10:**83-100.
40. **Levine, A. J.** 2009. The common mechanisms of transformation by the small DNA tumor viruses: The inactivation of tumor suppressor gene products: p53. Virology **384:**285-93.
41. **Li, H., A. V. Korennykh, S. L. Behrman, and P. Walter.** 2010. Mammalian endoplasmic reticulum stress sensor IRE1 signals by dynamic clustering. Proc Natl Acad Sci U S A **107:**16113-8.
42. **Li, Y., D. F. Boehning, T. Qian, V. L. Popov, and S. A. Weinman.** 2007. Hepatitis C virus core protein increases mitochondrial ROS production by stimulation of Ca2+ uniporter activity. FASEB J **21:**2474-85.
43. **Liddington, R. C., Y. Yan, J. Moulai, R. Sahli, T. L. Benjamin, and S. C. Harrison.** 1991. Structure of simian virus 40 at 3.8-A resolution. Nature **354:**278-84.

44. **Lilley, C. E., C. T. Carson, A. R. Muotri, F. H. Gage, and M. D. Weitzman.** 2005. DNA repair proteins affect the lifecycle of herpes simplex virus 1. Proc Natl Acad Sci U S A **102:**5844-9.
45. **Lin, H. J., R. H. Upson, and D. T. Simmons.** 1992. Nonspecific DNA binding activity of simian virus 40 large T antigen: evidence for the cooperation of two regions for full activity. J Virol **66:**5443-52.
46. **Low, J. A., B. Magnuson, B. Tsai, and M. J. Imperiale.** 2006. Identification of gangliosides GD1b and GT1b as receptors for BK virus. J Virol **80:**1361-6.
47. **Luo, Y., A. Y. Chen, and J. Qiu.** 2010. Bocavirus Infection Induces a DNA Damage Response That Facilitates Viral DNA Replication and Mediates Cell Death. J Virol.
48. **Machida, K., K. T. Cheng, C. K. Lai, K. S. Jeng, V. M. Sung, and M. M. Lai.** 2006. Hepatitis C virus triggers mitochondrial permeability transition with production of reactive oxygen species, leading to DNA damage and STAT3 activation. J Virol **80:**7199-207.
49. **Machida, K., K. T. Cheng, V. M. Sung, K. J. Lee, A. M. Levine, and M. M. Lai.** 2004. Hepatitis C virus infection activates the immunologic (type II) isoform of nitric oxide synthase and thereby enhances DNA damage and mutations of cellular genes. J Virol **78:**8835-43.
50. **Mercer, J., M. Schelhaas, and A. Helenius.** 2010. Virus entry by endocytosis. Annu Rev Biochem **79:**803-33.
51. **Moody, C. A., and L. A. Laimins.** 2009. Human papillomaviruses activate the ATM DNA damage pathway for viral genome amplification upon differentiation. PLoS Pathog **5:**e1000605.
52. **Nakanishi, A., J. Clever, M. Yamada, P. P. Li, and H. Kasamatsu.** 1996. Association with capsid proteins promotes nuclear targeting of simian virus 40 DNA. Proc Natl Acad Sci U S A **93:**96-100.
53. **Nakanishi, A., N. Itoh, P. P. Li, H. Handa, R. C. Liddington, and H. Kasamatsu.** 2007. Minor capsid proteins of simian virus 40 are dispensable for nucleocapsid assembly and cell entry but are required for nuclear entry of the viral genome. J Virol **81:**3778-85.
54. **Nakanishi, A., D. Shum, H. Morioka, E. Otsuka, and H. Kasamatsu.** 2002. Interaction of the Vp3 nuclear localization signal with the importin alpha 2/beta heterodimer directs nuclear entry of infecting simian virus 40. J Virol **76:**9368-77.
55. **Neu, U., T. Stehle, and W. J. Atwood.** 2009. The Polyomaviridae: Contributions of virus structure to our understanding of virus receptors and infectious entry. Virology **384:**389-99.
56. **Neu, U., K. Woellner, G. Gauglitz, and T. Stehle.** 2008. Structural basis of GM1 ganglioside recognition by simian virus 40. Proc Natl Acad Sci U S A **105:**5219-24.
57. **Orba, Y., T. Suzuki, Y. Makino, K. Kubota, S. Tanaka, T. Kimura, and H. Sawa.** 2010. Large T antigen promotes JC virus replication in G2-arrested cells by inducing ATM- and ATR-mediated G2 checkpoint signaling. J Biol Chem **285:**1544-54.

58. **Padgett, B. L., D. L. Walker, G. M. ZuRhein, R. J. Eckroade, and B. H. Dessel.** 1971. Cultivation of papova-like virus from human brain with progressive multifocal leucoencephalopathy. Lancet **1:**1257-60.
59. **Pallas, D. C., L. K. Shahrik, B. L. Martin, S. Jaspers, T. B. Miller, D. L. Brautigan, and T. M. Roberts.** 1990. Polyoma small and middle T antigens and SV40 small t antigen form stable complexes with protein phosphatase 2A. Cell **60:**167-76.
60. **Pelkmans, L., J. Kartenbeck, and A. Helenius.** 2001. Caveolar endocytosis of simian virus 40 reveals a new two-step vesicular-transport pathway to the ER. Nat Cell Biol **3:**473-83.
61. **Poulin, D. L., and J. A. DeCaprio.** 2006. Is there a role for SV40 in human cancer? J Clin Oncol **24:**4356-65.
62. **Rainey-Barger, E. K., B. Magnuson, and B. Tsai.** 2007. A chaperone-activated nonenveloped virus perforates the physiologically relevant endoplasmic reticulum membrane. J Virol **81:**12996-3004.
63. **Roederer, M., F. J. Staal, P. A. Raju, S. W. Ela, and L. A. Herzenberg.** 1990. Cytokine-stimulated human immunodeficiency virus replication is inhibited by N-acetyl-L-cysteine. Proc Natl Acad Sci U S A **87:**4884-8.
64. **Rohaly, G., K. Korf, S. Dehde, and I. Dornreiter.** 2010. Simian virus 40 activates ATR-Delta p53 signaling to override cell cycle and DNA replication control. J Virol **84:**10727-47.
65. **Ron, D., and P. Walter.** 2007. Signal integration in the endoplasmic reticulum unfolded protein response. Nat Rev Mol Cell Biol **8:**519-29.
66. **Rutkowski, D. T., and R. J. Kaufman.** 2004. A trip to the ER: coping with stress. Trends Cell Biol **14:**20-8.
67. **Sano, R., I. Annunziata, A. Patterson, S. Moshiach, E. Gomero, J. Opferman, M. Forte, and A. d'Azzo.** 2009. GM1-ganglioside accumulation at the mitochondria-associated ER membranes links ER stress to Ca(2+)-dependent mitochondrial apoptosis. Mol Cell **36:**500-11.
68. **Scheidtmann, K. H., M. C. Mumby, K. Rundell, and G. Walter.** 1991. Dephosphorylation of simian virus 40 large-T antigen and p53 protein by protein phosphatase 2A: inhibition by small-t antigen. Mol Cell Biol **11:**1996-2003.
69. **Schelhaas, M., J. Malmstrom, L. Pelkmans, J. Haugstetter, L. Ellgaard, K. Grunewald, and A. Helenius.** 2007. Simian Virus 40 depends on ER protein folding and quality control factors for entry into host cells. Cell **131:**516-29.
70. **Schreck, R., K. Albermann, and P. A. Baeuerle.** 1992. Nuclear factor kappa B: an oxidative stress-responsive transcription factor of eukaryotic cells (a review). Free Radic Res Commun **17:**221-37.
71. **Sen, C. K., S. Roy, and L. Packer.** 1996. Involvement of intracellular Ca2+ in oxidant-induced NF-kappa B activation. FEBS Lett **385:**58-62.
72. **Shi, Y., G. E. Dodson, S. Shaikh, K. Rundell, and R. S. Tibbetts.** 2005. Ataxia-telangiectasia-mutated (ATM) is a T-antigen kinase that controls SV40 viral replication in vivo. J Biol Chem **280:**40195-200.

73. **Simmen, T., E. M. Lynes, K. Gesson, and G. Thomas.** 2010. Oxidative protein folding in the endoplasmic reticulum: tight links to the mitochondria-associated membrane (MAM). Biochim Biophys Acta **1798:**1465-73.
74. **Stehle, T., S. J. Gamblin, Y. Yan, and S. C. Harrison.** 1996. The structure of simian virus 40 refined at 3.1 A resolution. Structure **4:**165-82.
75. **Sullivan, C. S., A. T. Grundhoff, S. Tevethia, J. M. Pipas, and D. Ganem.** 2005. SV40-encoded microRNAs regulate viral gene expression and reduce susceptibility to cytotoxic T cells. Nature **435:**682-6.
76. **Suzuki, T., Y. Orba, Y. Okada, Y. Sunden, T. Kimura, S. Tanaka, K. Nagashima, W. W. Hall, and H. Sawa.** 2010. The human polyoma JC virus agnoprotein acts as a viroporin. PLoS Pathog **6:**e1000801.
77. **Tardif, K. D., G. Waris, and A. Siddiqui.** 2005. Hepatitis C virus, ER stress, and oxidative stress. Trends Microbiol **13:**159-63.
78. **Tsai, B., J. M. Gilbert, T. Stehle, W. Lencer, T. L. Benjamin, and T. A. Rapoport.** 2003. Gangliosides are receptors for murine polyoma virus and SV40. EMBO J **22:**4346-55.
79. **Vembar, S. S., and J. L. Brodsky.** 2008. One step at a time: endoplasmic reticulum-associated degradation. Nat Rev Mol Cell Biol **9:**944-57.
80. **Waris, G., A. Livolsi, V. Imbert, J. F. Peyron, and A. Siddiqui.** 2003. Hepatitis C virus NS5A and subgenomic replicon activate NF-kappaB via tyrosine phosphorylation of IkappaBalpha and its degradation by calpain protease. J Biol Chem **278:**40778-87.
81. **Weitzman, M. D., C. E. Lilley, and M. S. Chaurushiya.** 2010. Genomes in conflict: maintaining genome integrity during virus infection. Annu Rev Microbiol **64:**61-81.
82. **Wu, C., R. Roy, and D. T. Simmons.** 2001. Role of single-stranded DNA binding activity of T antigen in simian virus 40 DNA replication. J Virol **75:**2839-47.
83. **Wu, Z. H., Y. Shi, R. S. Tibbetts, and S. Miyamoto.** 2006. Molecular linkage between the kinase ATM and NF-kappaB signaling in response to genotoxic stimuli. Science **311:**1141-6.
84. **Yu, X., C. C. Chini, M. He, G. Mer, and J. Chen.** 2003. The BRCT domain is a phospho-protein binding domain. Science **302:**639-42.
85. **Zhang, K., and R. J. Kaufman.** 2008. From endoplasmic-reticulum stress to the inflammatory response. Nature **454:**455-62.
86. **Zhao, X., R. J. Madden-Fuentes, B. X. Lou, J. M. Pipas, J. Gerhardt, C. J. Rigell, and E. Fanning.** 2008. Ataxia telangiectasia-mutated damage-signaling kinase- and proteasome-dependent destruction of Mre11-Rad50-Nbs1 subunits in Simian virus 40-infected primate cells. J Virol **82:**5316-28.